Quantitative Risk Analysis of Fracture Propagation from Salt Cavern ZW-03

Final Report for Nobian EnergyStock

Fenix Consulting Delft BV
5.1.2.e , 5.1.2.e

Date
July 2024

Quantitative Risk Analysis of Fracture Propagation from Salt Cavern ZW-03

Final Report for Nobian EnergyStock

Date
July 2024

DISCLAIMER

Fenix Consulting Delft nor any person acting on behalf of Fenix:

- **Makes any warranty or representation, express or implied, with respect to the accuracy, completeness, or usefulness of the information contained in this report, or that the use of any apparatus, method, or process disclosed in this report may not infringe privately owned rights; or**

- **Assumes any liability with respect to the use of, or for damages resulting from the use of, any information, apparatus, method, or process disclosed in this report.**

Executive Summary

Salt solution mining creates large caverns that are abandoned after a suitable waiting period after mining is stopped. The waiting period allows for the temperature of the brine to increase towards the temperature of the surrounding rock salt. The initial convergence of the cavern occurs during the waiting period, before the well is sealed, so that any increase in pressure can be bled off at the surface. Once the cavern is permanently sealed, it is foreseen that the pressure of the brine in the cavern rises to a high level due to continued convergence of the cavern caused by salt creep. The pressure at the top of the cavern may exceed the stress in the salt so that a hydraulic fracture can be initiated and propagated upwards.

Virgin permeability of salt is extremely low, but the simulation of cavern convergence due to creep yields a zone of much higher permeability above the cavern. Brine at high pressure permeates upwards through this zone, giving a high pore pressure that exceeds the stress. With a negative effective stress, it is expected that open micro-fractures exist in the salt (corresponding to the high permeability). This makes it likely that fracture initiation can occur at relatively low pressures, without having to exceed any "breakdown" pressure that is normally higher than the minimum stress.

A standard industry fracture simulator is used to estimate the fracture dimensions when a fracture initiates and brine flows out of the cavern into the fracture. The boundary condition for fracture propagation is the cavern pressure. In turn, the cavern pressure decreases due to the fluid flow into the fracture, as given by the cavern compressibility.

For an overpressure of 15bar above the minimum stress at the borehole plug, the fracture is assumed to propagate and the volume of brine that flows from the cavern before the pressure falls to the minimum stress level is about 3500m3. Even for a fluid volume of 1000m3, the fracture could potentially propagate through the salt and reach the North Sea overburden formation.

Conclusions

- A volume of 1000m3 is sufficient to propagate a fracture through the salt to reach the permeable overburden (North Sea formation) for this cavern.
- The elevated pore pressure in the salt volume above the cavern results in a very small difference in pressure between the fluid in the fracture and the pore fluid, which leads to very low fluid leak-off from the fracture, so that a large fracture will be propagated.
- Compressibility of the pore fluid in the salt is the most important parameter that determines fluid leak-off from the fracture. If the pores are filled with brine, the compressibility is quite low, giving low fluid leak-off. Much more leak-off could result if there is some gas saturation, giving a much higher compressibility for the pore fluid.
- If a significant fracture has propagated from the cavern (but still stays within the salt) the brine permeation is enhanced by 2.5m3/day due to leak-off from the fracture. This results in a lower cavern pressure that might result in a stable fracture that does not propagate further.

Contents

List of Figures

Nomenclature

Units: SI (m= metre, s= second, kPa =10^3Pa, MPa =10^6Pa, GPa =10^9Pa)

Dimensions: m= mass, L= length, t= time

Variable		Description	Units	Dimensions
A_p	:	Poroelastic coefficient	[-]	(-)
K_T	:	Thermal Conductivity	[W/mK]	(m/Lt^2)
K_D	:	Permeability	[m2]	(L^2)
C_p	:	Heat Capacity	[J/kgK]	(m/Lt^2)
E	:	Young's modulus	[GPa]	(m/Lt^2)
G	:	Stress gradient	[kPa/m]	(m/L^{2}t^2)
p	:	pressure	[MPa]	(m/Lt^2)
α_B	:	Biot coefficient	[-]	(-)
ν	:	Poisson's ratio	[-]	(-)
ϕ	:	Porosity	[-]	(-)
$\sigma_{H,max}$	:	maximum horizontal stress	[MPa]	(m/Lt^2)
$\sigma_{h,min}$	:	minimum horizontal stress	[MPa]	(m/Lt^2)
σ_{vert}	:	vertical stress	[MPa]	(m/Lt^2)

1 Introduction

In the Zuidwending area, Nobian has been mining salt by solution mining since the 1960's. Safe operation of the caverns within an acceptable operating window for the pressure is secured while the boreholes remain open and pressure control is possible. This may change after cavern abandonment when the borehole is permanently closed by placing a plug in the wellbore at some distance above the cavern roof.

Recent scientific advances have indicated that the long-term behavior of the caverns is governed by pressure solution creep. With that mechanism considered, the pressure build-up inside caverns after abandonment may be greater than previously calculated. At high cavern pressure it is expected that the mechanism of flow into a permeable porous medium is possible and will cause some pressure relief by infiltration of brine into the salt formation. Considering all effects controlling the long-term cavern pressure after abandonment in the Zuidwending field, it is possible that permeable flow is insufficient to keep the pressure below fracture initiation pressure.

One of the possible effects if the pressure increases too much is that a hydraulic fracture initiates in the subsurface at the lowermost abandonment plug depth, along which brine could flow upward. Fracture growth could potentially be limited to stay within the rock salt formation, or could reach the permeable overburden layer where significant fluid leak-off would occur, which may stabilize the situation by means of fracture arrest. However, continued upward fracture growth through the overburden layer could result in contamination of fresh groundwater sources.

This report presents an analysis of potential fracture propagation based on the FEM cavern convergence modeling that was performed by other consultants (Brouard, 2024). The predictions of fracture propagation shown in this report can be used to determine the cavern abandonment strategy, which is necessary for the permit applications.

2 Properties of the salt and overburden.

For modeling the potential fracture initiation and propagation it is necessary to populate the fracturing model with the stress, stiffness, permeability, porosity and pore pressure of overburden layers in order to estimate the upward fracture growth. These data were provided by Nobian.
Of particular interest is the minimum horizontal stress at the top of the cavern in the salt, since that will determine the potential for fracture initiation and fluid flow out of the cavern.

Table 1: Properties of the formation layers. The Halite layers have a very low virgin permeability, which is however enhanced when the halite undergoes plastic deformation due to cavern convergence and subsidence.

Layer	Top (m)	Thickness (m)	Density (kg/m3)	E (GPa)	ν (-)	K_T (W/m/K)	Cp (J/kg/K)	ϕ (BV)	K_D (mD)
Miocene	0	129	2300	1	0.3	2.4	857	10	100
Cretaceous	129	10	2200	9	0.3	2.5	857	10	10
Triassic	139	21	2450	10	0.3	3.2	857	10	20
ZEZ2HL2-HU	160	917	2165	33	0.25	5.8	750	0.1	1.0E-06
ZEZ3	1077	750	2165	33	0.25	5.8	750	0.1	1.0E-06
ZEZ2HL2-HU	1827	173	2165	33	0.25	5.8	750	0.1	1.0E-06

Table 2: Parameters of the ZW-03 cavern.

ZW-03		
Compressibility	3.89E-10	1/Pa
Volume	6.34E+06	m3
Cavern compressibility	2.47E+02	m3/bar
Minimum Stress at plug	90.3	bar

The FEM model, using axial symmetry, developed by Brouard (2024) will provide the stress in the rock salt and the overburden over time. When the pressure in the cavern rises sufficiently, the pressure at the top of the cavern might exceed the minimum horizontal stress in the rock salt so that a fracture can initiate. The fracture nucleation process is quite complex, but for practical purposes a simple criterion will be used based on minimum horizontal stress.

The size of the fracture depends on leak-off to the rock layers and the balance between fluid pressure and rock stress. It is likely that the initial fracture propagation will be governed by the mass balance between brine volume due to fast decompression of the cavern and propagating fracture volume, because initially the brine pressure will be much higher than the minimum horizontal stress in the overburden. Long-term behaviour (several years) will be governed by the balance between cavern convergence and fracture leak-off and fracture storage. The wellbore diagram of the ZW-03 cavern is shown in Figure 1. The roof of the cavern is kept at a depth of 470m, so that the plug might be put 50m above the roof at a depth of 424m.

The cavern will be mined until 2040, after which a wait period of 50 years is foreseen after which the borehole will be plugged and the cavern pressure will rise to a maximum pressure at the roof of 129bar in 2097, resulting in a maximum pressure of 120bar at the plug, shown in Figure 2. For a very long time, the pressure will remain at an elevated level above the minimum stress of 90.3bar at the plug.

The mechanical and hydraulic properties of the formation are derived from the cavern simulation, by averaging the properties over a zone of 100m from the borehole or cavern wall. The result is shown in Figure 3. Fluid permeation from the cavern is possible because the salt permeability is enhanced by dilation due to plastic deformation. Remarkably, the pore pressure in the salt is higher than the minimum stress. This situation remains stable since the stress becomes isotropic so that shear deformation is impossible. Figure 4 shows the pore pressure and stress at the point of fracture initiation vs. distance from the borehole. Only far from the borehole does the pore pressure fall back to hydrostatic level and the permeability falls to the virgin value.

The pressure and stress on the cavern wall are plotted in Figure 6. Since the stress gradient is much larger than the pressure gradient, the high pressure induced by cavern convergence gives a pressure near the cavern roof that exceeds the minimum stress.
Note that the stress shows some fluctuations that are caused by very high stress in some elements that are strongly deformed. The largest singularities were removed, but some fluctuations remained around the deformed elements.

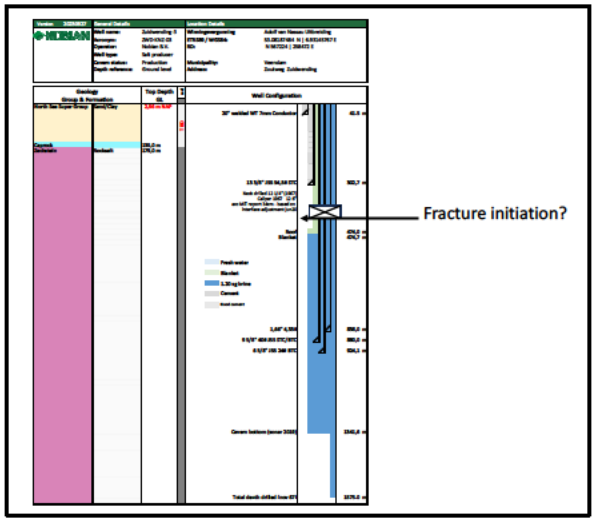

Figure 1: Wellbore diagram of ZW-03 borehole. All depths in the report are referred to Ground Level.

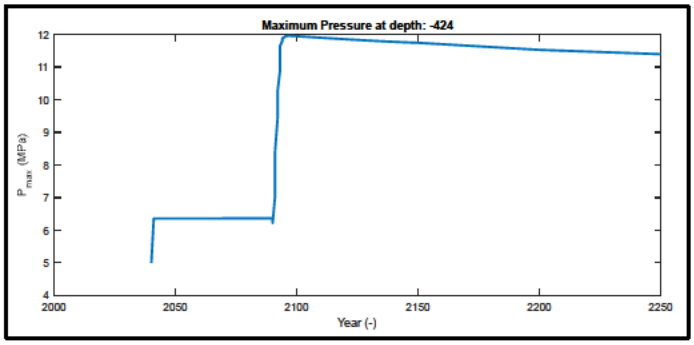

Figure 2: Maximum pressure at a depth of 424m (TVDGL) vs time.

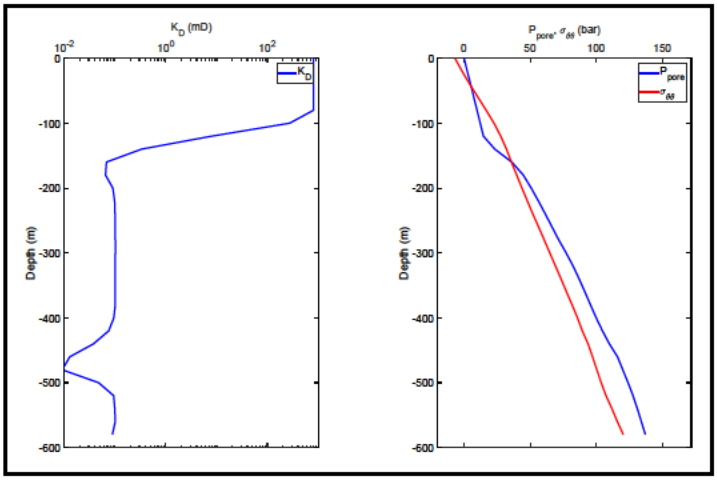

Figure 3: Formation properties vs depth derived from the cavern simulation at the time of maximum pressure in 2097.

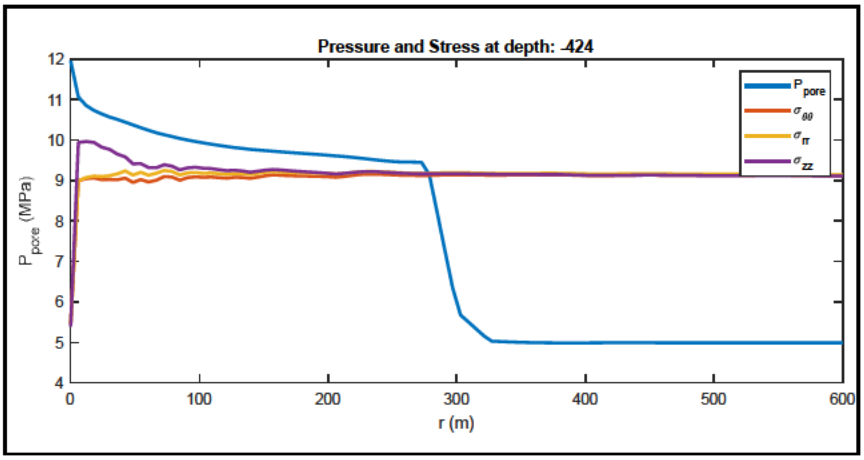

Figure 4: Simulated pore pressure and stress vs radial distance from the borehole in 2097.

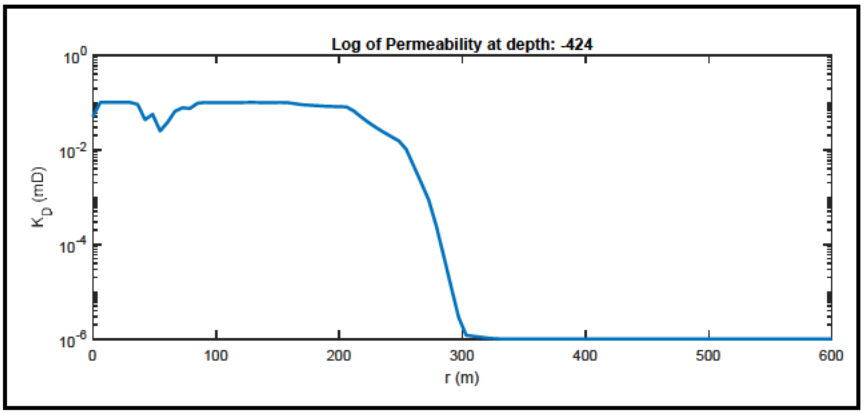

Figure 5: Permeability vs radial distance from the borehole in 2097.

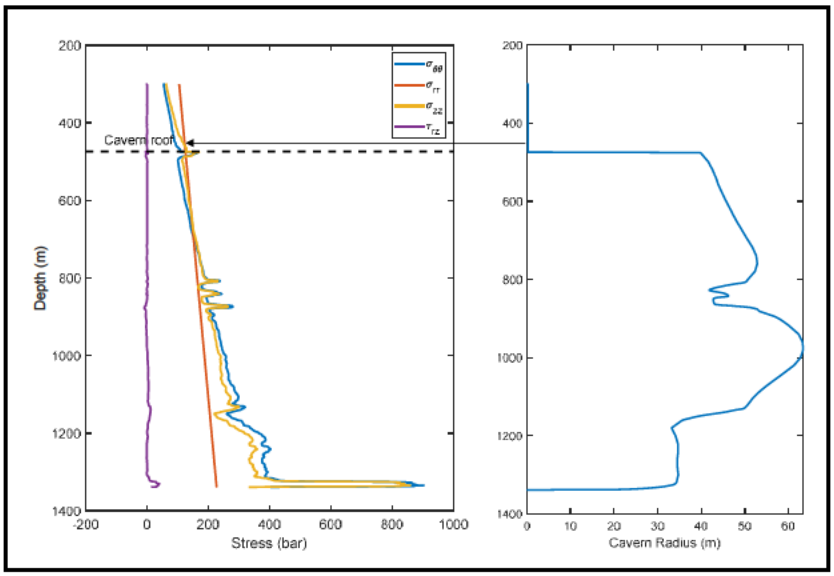

Figure 6: Left: Simulated stress and pressure vs depth in 2097. Fracture initiation becomes possible at the top since pressure (equal to radial stress) exceeds the minimum stress. Right: Cavern radius vs depth.

3 Modeling fracture initiation with sensitivities

Fracture simulation model

We used a pseudo-3D fracture simulator (Cleary *et al*., 1986). The simulator is based on solving the mass balance and elastic fracture opening by using a formation model, including stress, permeability and stiffness to compute the fracture geometry. The geometry is simplified to an upper ellipse and a lower ellipse. The pressure and width profile along the fracture are captured with functional coefficients. Normally, the simulator is run from a flow rate boundary condition, but in this case the pressure of the cavern acts as boundary condition. By adjusting the injection rate, the simulated pressure is matched to the cavern pressure that falls due to the resulting flow from the cavern into the fracture. In hydraulic fracturing for well stimulation, the fracture height is governed by the stress difference between the reservoir and overburden. In the salt formation, stress changes almost linearly with depth and the fracture height is determined by the balance between the fluid pressure gradient in the fracture and the stress gradient of the rock salt. Since stress changes more than fluid pressure with depth, the fracture will tend to grow upwards and the only limitation on the fracture height growth is the amount of fluid available from the cavern depressurization.

For the simulations we need formation permeability, the modulus and minimum horizontal stress as a function of depth, which are obtained from the cavern simulation (Brouard, 2024).

Breakdown and fracture initiation

Measuring breakdown and stress in micro-frac tests in salt formations is complicated due to creep and plastic behaviour of the salt and small leaks that apparently occur at the packers (Rummel *et al*., 1996; Schmidt1993). Some tests indeed show the flat pressure response upon shut-in that is expected if the salt has a permeability of 1 nD, but many tests show rapid pressure decline that would indicate a high permeability of about 1mD or a leakage along the straddle packers used for micro-frac tests. Wawersik (1989) showed with FEM analysis that creep has a major influence on the test results and that even a short time after drilling the stress concentration around the wellbore dissipates so that standard elastic breakdown theory is invalid. The result is that a fracture can already initiate below minimum stress and propagate at a pressure a little bit above the minimum stress.

Furthermore, it will be shown that the simulations of cavern convergence yield a pore pressure and elevated permeability above the cavern so that fracture initiation should happen at low pressure, since the negative effective stress results in open micro-fractures that can accept fluid flow.

There is uncertainty about the cavern convergence simulations, although the constitutive behaviour has been calibrated on field experiments, but it would be too optimistic to assume a large breakdown pressure gradient of 25-30kPa/m as has been observed in some micro-frac tests. Of course, fracture propagation requires fluid flow and overcoming the fracture tip resistance, resulting in a net pressure of about 15bar. For the depth of the ZW-03 cavern roof, this corresponds to a pressure gradient of about 25.0kPa/m, assuming a minimum stress gradient of 21.5kPa/m.

Fracture simulation of initial propagation with Fracpro

Fracture propagation is coupled to cavern behaviour that depends on the pressure in the cavern. Given all uncertainties it is more practical to use a separate fracture simulation that models the fracture growth based on the volume that is expelled by the cavern. The industry-standard Fracpro simulator will be used for this simulation which will provide sufficient accuracy to make a reliable estimate of the fracture growth. The goal of these simulations is to make a clear distinction between a regime where the fracture is just a few hundreds of meters high compared with a regime where the fracture can reach shallow layers (at 150m depth).

The fracture simulator will be coupled to the FEM model of the cavern by the fluid loss and fluid pressure of the cavern. The fracture simulator uses flow rate as input and computes pressure in the fracture that is coupled back to the cavern model. The cavern convergence for a given brine pressure then delivers the flow rate for the fracture model.

The most important sensitivities will be abandonment plug depth, rate of convergence and the stress and properties of the formation near the cavern. The stress near the cavern will be used, but any interaction of the fracture with the cavern will be neglected.

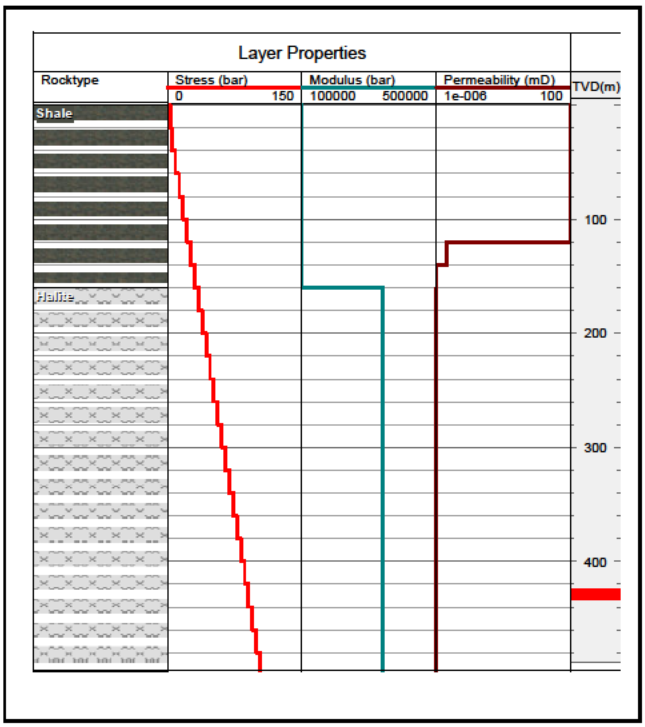

Figure 7: Layer properties used in the Fracpro simulations; depth is TVDGL.

The initial fracturing pressure was taken at 106bar at the fracture initiation point at a depth of 424m. The fracture simulator works from the specified injection rate, which was adjusted over time so that the injection pressure matched the cavern pressure that is falling with injection volume, see Figure 8. The injection rate is shown in Figure 9.

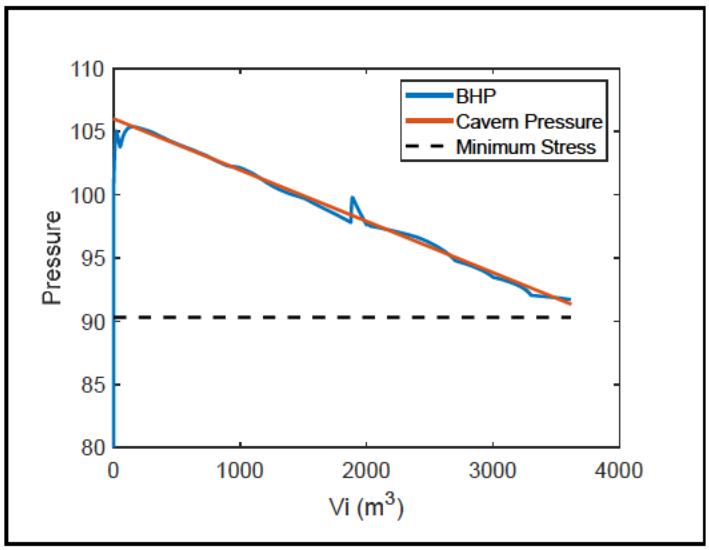

Figure 8: Fracpro simulation of BHP vs injected volume. The cavern pressure is computed with the volume loss and the compressibility of the cavern.

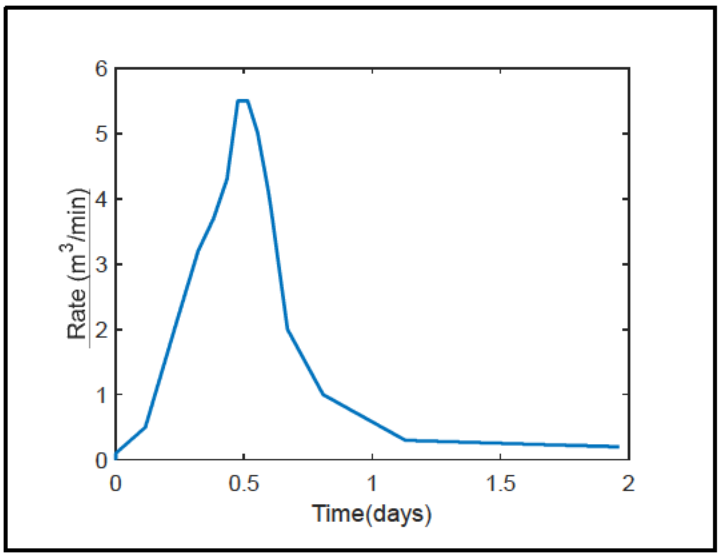

Figure 9: injection rate vs time.

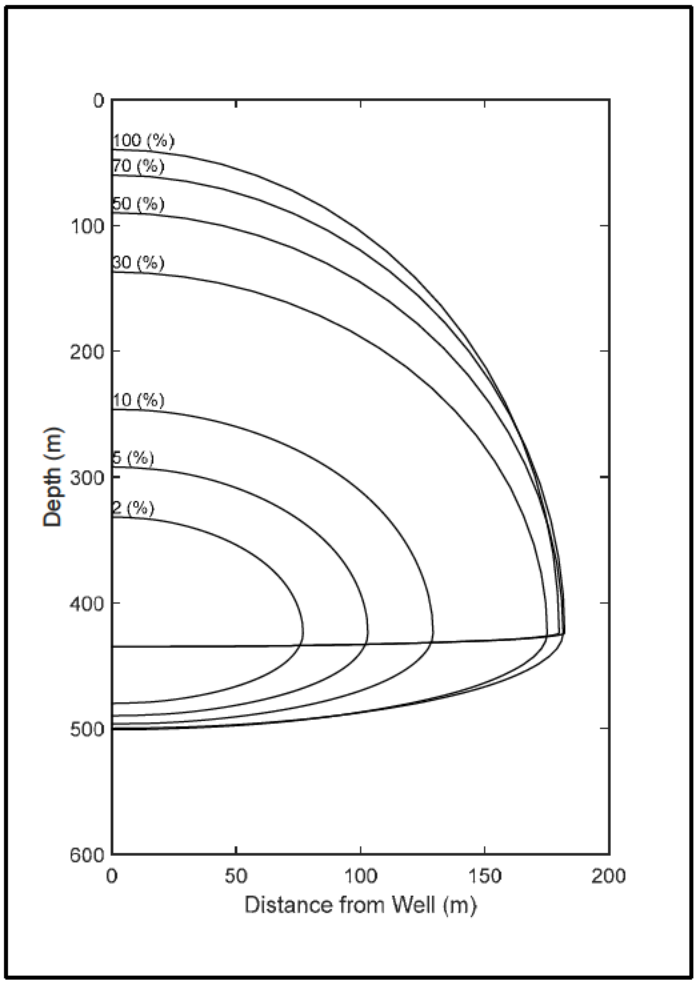

Figure 10: Simulated fracture profile for different injection volumes (given as a percentage of total volume). At the end, the lower part of the fracture closes due to the lower pressure.

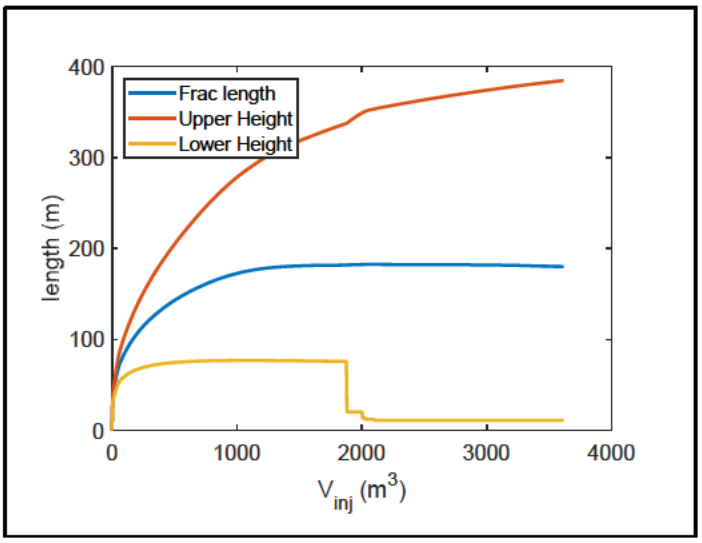

Figure 11: Simulated fracture length and height vs time.

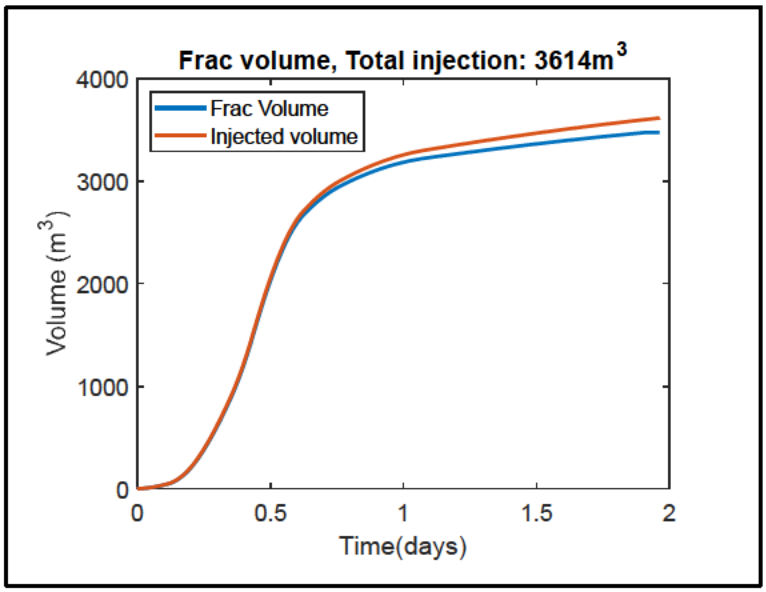

Figure 12: Simulated fracture volume and injected volume vs time.

Figure 10 shows the subsequent fracture profiles for different injection volumes (given as a percentage of total volume). It is seen that the fracture already reaches the North Sea formation at 30% of the total injected volume, so when the fracture pressure is still much higher than the minimum stress. The fracture shape is described with two quarter ellipses given by the fracture length, an upper height and a lower height that are plotted vs time in Figure 11. Figure 12 shows that the fracture volume initially follows the injected volume and fluid leak-off from the fracture only starts after the fracture reaches the North Sea formation.

The most critical parameter for leak-off in a saturated formation is the compressibility of the pore fluid, which determines the storage capacity. It was assumed that the compressibility is very low since there is no evidence of gas saturation in the salt. However, even a small gas saturation in the salt would give much higher compressibility. Therefore, a simulation was run with 100 times higher compressibility which indeed gives more leak-off as shown in Figure 13 and Figure 14.

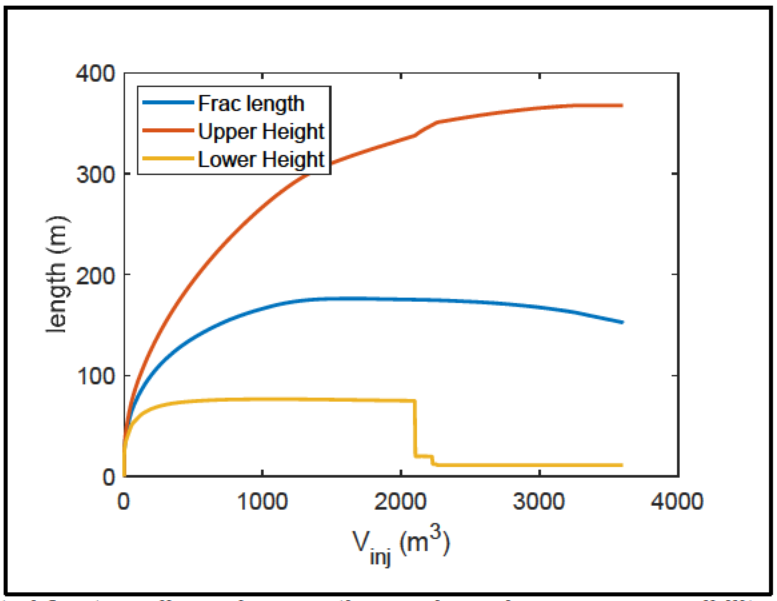

Figure 13: Simulated fracture dimensions vs time, using a larger compressibility which gives more fluid leak-off.

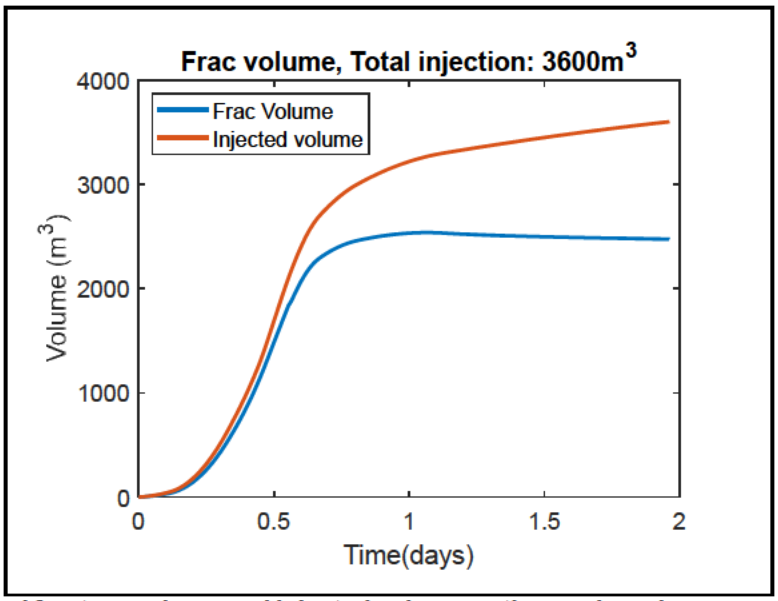

Figure 14: Simulated fracture volume and injected volume vs time, using a larger compressibility which gives more fluid leak-off. The total injection volume was slightly lower due to the approximation of the pressure decline by adjusting the rate over time, but the effect is insignificant.

FEM simulation of fracture growth

The fracture simulations are based on a number of assumptions, such as simplified geometry and an infinite formation that might lead to inaccuracies in the predictions. Therefore, we confirmed the simulations with a full 3D fracture simulation that models a fracture in a rock mass including the free surface. Fracture propagation is governed by effective tensile strength (of 2 MPa – 20 bar) at the fracture tip and Darcy leak-off from the fracture, which is of course very low in salt. The tensile strength is a bit higher than the net pressure that resulted in the Fracpro simulations, but these models are different since the FEM model uses effective stress. The tensile strength of 2MPa is modest and the resulting net pressure depends on the entire fracture opening that is computed.

Figure 15 shows the FEM model with a fracture during the simulation. For each time step, the leak-off and fracture pressure is computed; the fracture opening is based on the pressure profile.

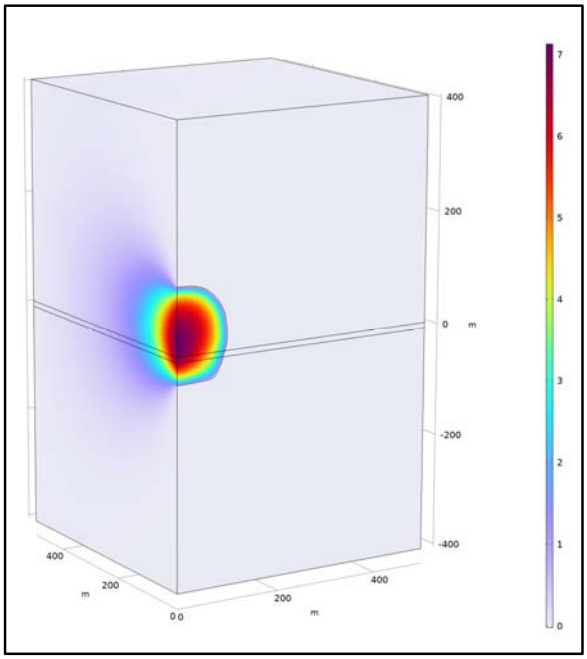

Figure 15: Fracture width shown in FEM of fracture propagation in a salt formation. The width scale is in mm. The black lines indicate the initial fracture location, at a depth of 424m.

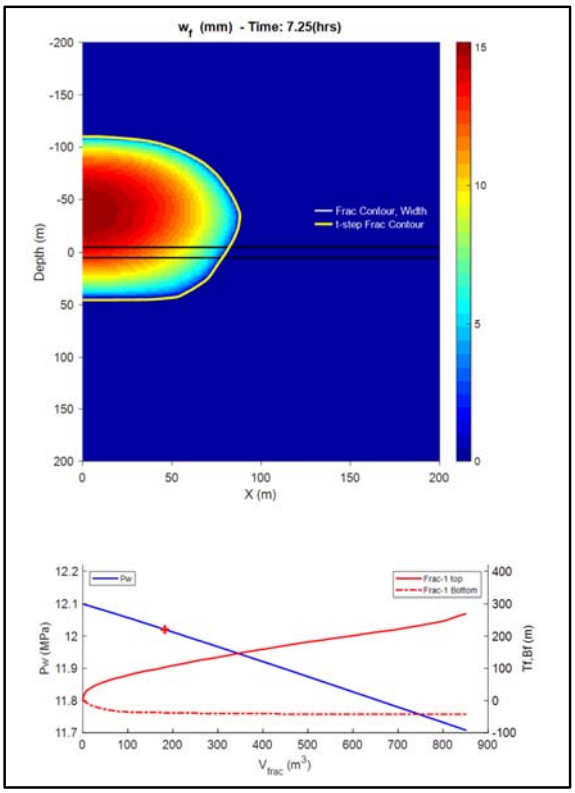

Figure 16: Fracture width contours after 7.25 hrs (upper) and cavern pressure and fracture upper and lower height vs injection volume (lower). The red cross indicates the pressure and volume for the upper plot.

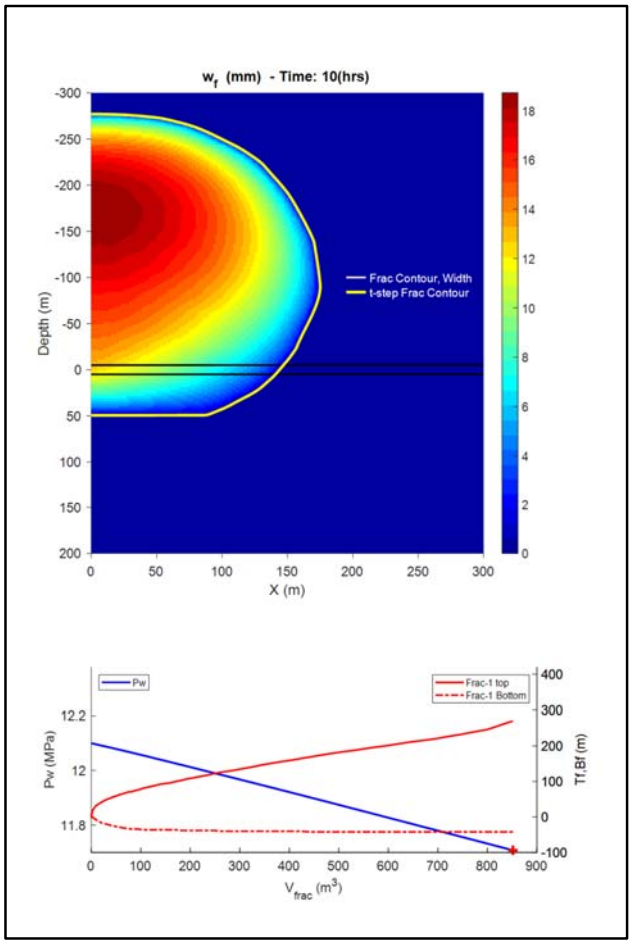

Figure 17: Fracture width contours after 10hrs (upper) and cavern pressure and fracture upper and lower height vs injection volume (lower). The red cross indicates the pressure and volume for the upper plot.

Figure 16 and Figure 17 show the Fracture geometry and width. There are some differences with the Fracpro simulation results, but the fracture height and injection volume agree: the 3D model predicts that the fracture reaches the North Sea formation for an injection volume of 850m^3.

4 Potential for long-term fracture propagation

The potential fracture growth out of the salt formation may be unacceptable, so that a solution should be found to mitigate fracture size. Filling the cavern partially with a granular solid will reduce cavern compressibility and also the volume that would flow into a fracture. The question then arises if a stable situation would be attained if a smaller fracture grows with continued convergence with a partially filled cavern.

Fracture fluid leak-off

First, a smaller fracture is considered that remains within the salt formation. For an injection volume of 380m3 the fracture remains inside the salt formation. This volume is smaller than what was observed in the simulation with an injection volume of 3600m3, since there is considerable fracture growth after stopping injection. This happens since the high-pressure fluid can flow upward and further propagate the fracture during pressure equilibration when injection ceases.

Figure 18 shows the fracture profiles for such a smaller fluid volume. The next question is what level of leak-off can be expected. This was computed by adding a shut-in period of a few days to the fracture simulation.

Figure 19 shows the leak-off rate which reaches a value of 0.6m3/day. Over time the leak-off rate even falls again since the fracture is closing at the fracture entry point, which gives smaller leak-off because the pressure differential with the formation falls. The computed leak-off is quite small and it would take a long time for the fracture to close. The low leak-off is caused by persistent high pore pressure in the formation and the assumed low compressibility of the pore fluid in the salt.

Also, the leak-off computation considers only the fracture while the fluid flow from the cavern-fracture system is clearly coupled. Therefore, the combined system will also be used for estimating leak-off in the next section.

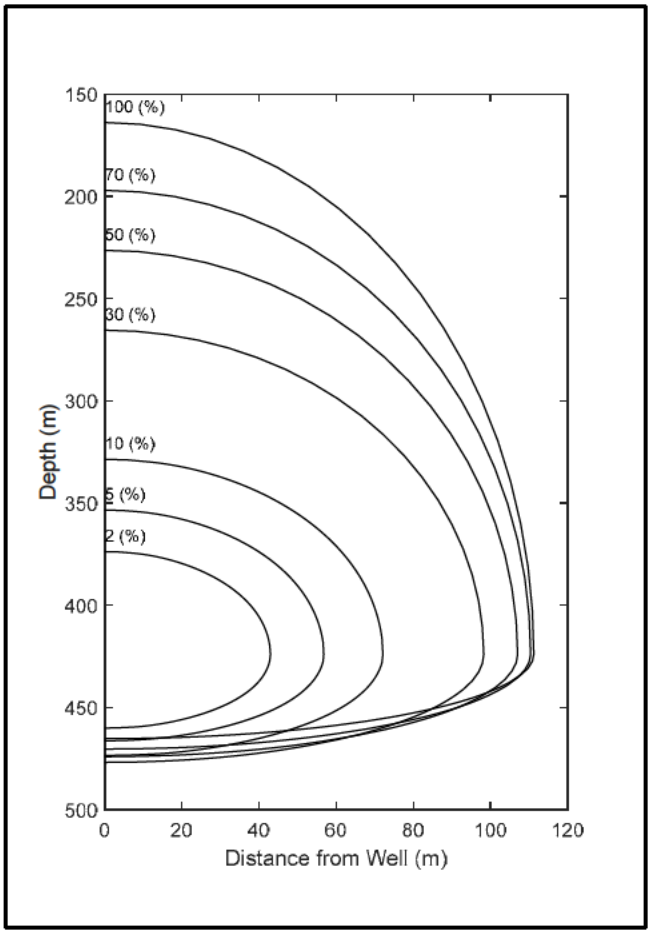

Figure 18: Simulated fracture profile for different injection volume (given as percentage of total volume) for a smaller fluid volume of 380m3.

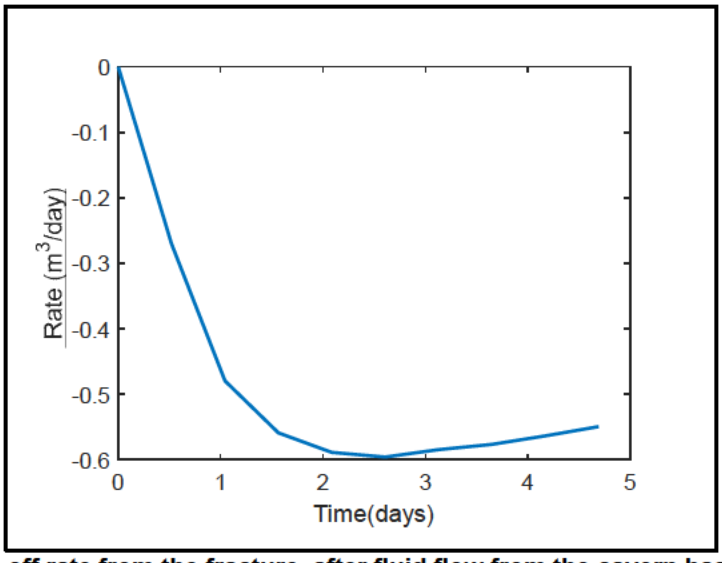

Figure 19: Fluid leak-off rate from the fracture, after fluid flow from the cavern has stopped. With such a low leak-off rate it would take years for the fracture to close.

Fracture-Cavern Permeation

The long-term pressure behaviour in this cavern shows persistent high pressure above the cavern. The question is: "Whether a fracture that would still be contained within the salt might still grow out of the salt due to the high cavern pressure?". The cavern simulations show a steady permeation from the cavern, so the fracture propagation could only be arrested if the additional permeation from the fracture faces would cause a significant pressure drop in the cavern. The fracture simulator is not suited to compute the permeation from the fracture in this case with a very high pore pressure in the formation. Therefore, a FEM simulation is used to compare the permeation from the cavern with the permeation from a cavern-fracture system using Darcy flow both in the rock mass as well as the fracture.

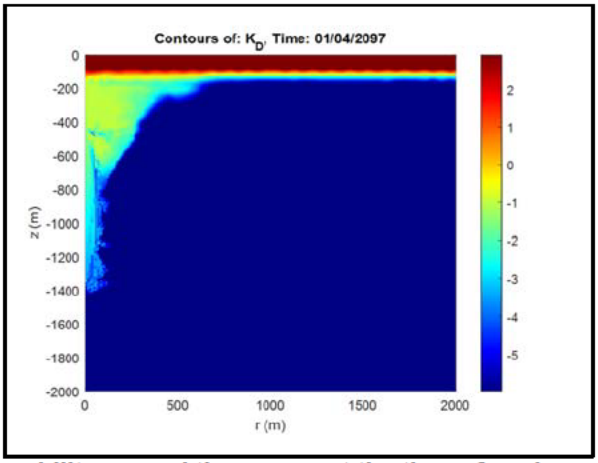

Figure 20: Simulated permeability around the cavern at the time of peak pressure.

The salt formation is modeled in quarter symmetry with a 2km x 2 km block. The overburden has a high permeability and the virgin permeability of the salt is very low. However, cavern convergence causes dilation and micro-fracturing above the cavern, which is taken from the cavern simulation (see Figure 20) and applied

in the FEM model with a cavern that is modeled as a cylinder and a penny-shaped fracture that is just connected to the top of the cavern, see Figure 21. The logarithm of permeability is shown in Figure 22.

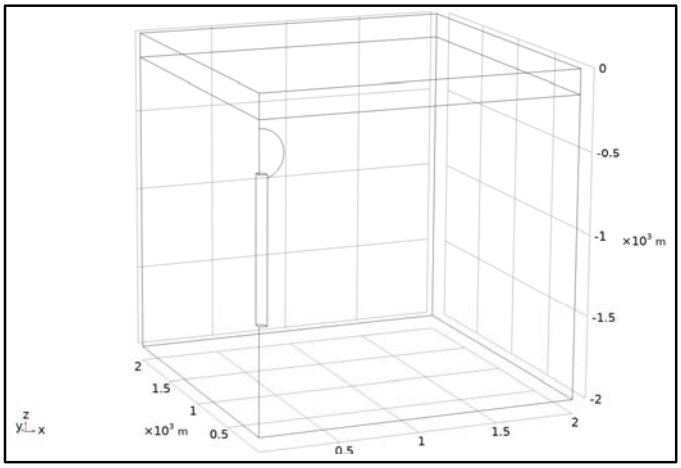

Figure 21: Model of Cavern with fracture

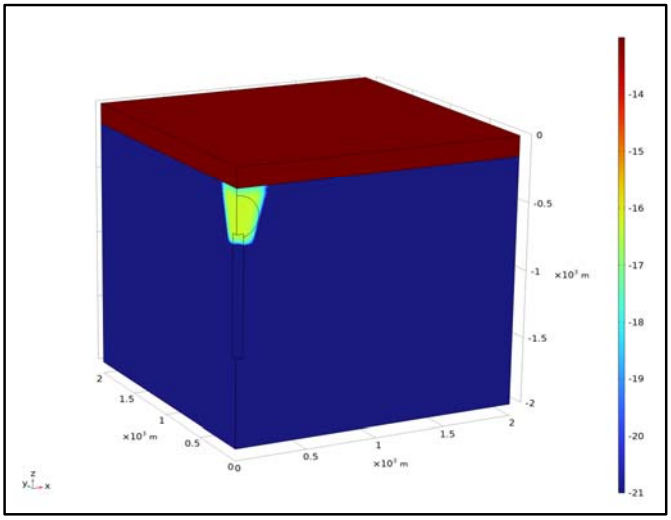

Figure 22: Logarithm of permeability (in m^2) in the FEM model for simulating cavern-fracture permeation.

By applying the cavern pressure on the cavern wall, the resulting pressure is shown in Figure 23, where the fracture conductivity is set to the virgin salt permeability so that it will not contribute to permeation. For this situation, the model gives a permeation rate of $4.3m^3$/day, which agrees approximately with the cavern simulation. Figure 24 shows the pressure and stress along a line on the cavern wall through the fracture.

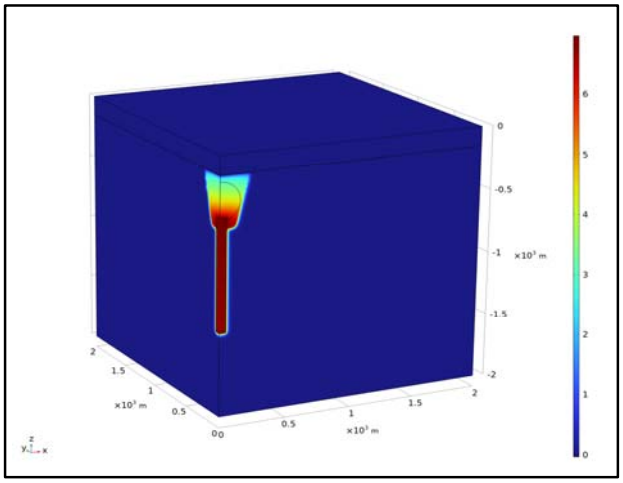

Figure 23: Simulated pressure (in MPa) above the cavern when the pressure in the cavern is defined by the cavern simulation the time of peak pressure in 2097. The fracture conductivity is set to zero.

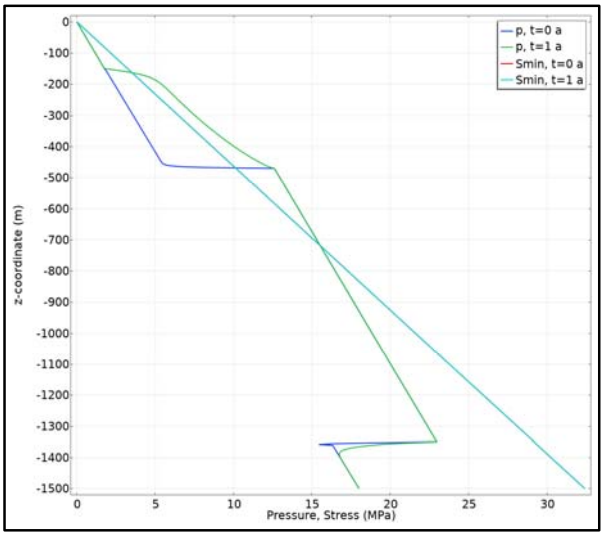

Figure 24: Pressure profile along the cavern through the fracture that approximates the pressure in the cavern simulation with higher pore pressure above the cavern compared with the stress.

If the fracture conductivity is set to a very high level, corresponding to an open fracture, the pressure profile is a bit different, as shown in Figure 25 and Figure 26. It is found that the permeation rate is increased to 6.8m^3/day. This additional flow would indeed result in a slow reduction in the cavern pressure of 1bar per 100 days.

The cavern convergence simulations show a range of permeation rates resulting in different pressures. That would indicate a significant effect on cavern pressure, but it would be necessary to confirm this with a simulation including the effect of additional fluid loss from the cavern.

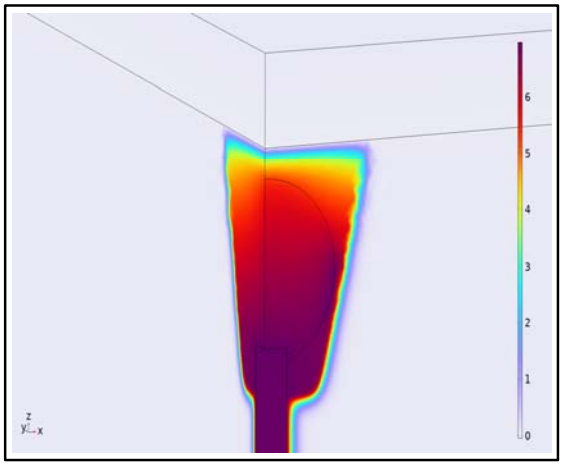

Figure 25: Pressure above the cavern (in MPa) with a conductive fracture.

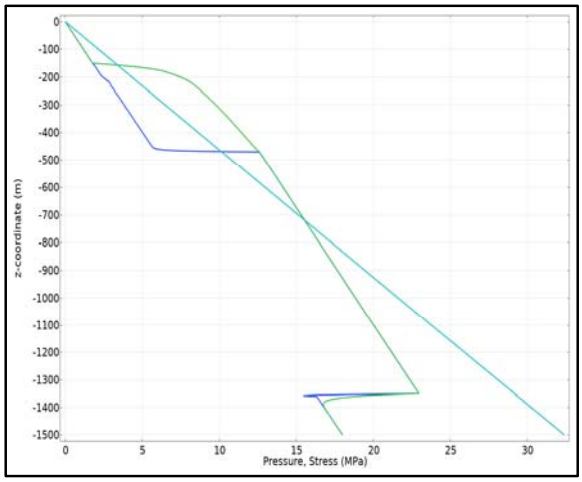

Figure 26: Pressure profile along the cavern and through the fracture. Due to the conductive fracture, the pressure is somewhat higher above the cavern compared with the situation without a fracture.

Discussion and Conclusions

Safe abandonment of the salt cavern requires that the potential propagation of a hydraulic fracture is predicted. The first question is: "At what pressure a fracture could propagate and what size the fracture might reach?". In fracturing tests such as micro-fracs, the peak pressure may be quite high, but that is in virgin salt whereas the salt formation is modified by the cavern operation and abandonment. In particular, the dilation zone above the cavern (where the fracture is expected to propagate) has much higher permeability and pore pressure. Those conditions are quite different from the formation properties in which fracture tests have been conducted. However, from research on fracture initiation in rock, it has been found that breakdown should be easy with many open micro-fractures in the salt above the cavern.

Therefore, we assumed that a fracture could initiate easily without a large breakdown effect, which resulted in a fracture initiation gradient of 25kPa/m. The size of the fracture is governed by the pressure reduction of the cavern due to brine flow. For the very large ZW-03 cavern with a pressure reduction of 1bar per 240m3 this yields a large volume of fluid that can flow into the fracture so that the fracture could reach the North Sea formation above the salt.

Fracture propagation in rock formations is uncertain, since the fracture propagation pressure cannot be accurately predicted. Furthermore, fracture height growth is quite uncertain. Lamination and other heterogeneities play a large role in these uncertainties. Although rock salt is relatively uniform compared with normal sand-shale formations, there are some laminations with different properties in the Zechstein salts. For

safety (most conservative assumptions), the simulations assumed a fairly low propagation pressure and no containment of the fractures. In this sense, the simulation results represent a worst-case scenario. Fracture height growth is uncertain, but there is no obvious, reliable barrier in the salt formation that could arrest fracture propagation.

Under normal conditions, only strong stress barriers (like Zechstein salts) or high-permeability layers can be counted on as reliable barriers. The salt itself has no strong barriers and under virgin conditions permeability is negligible. Above the cavern, a significant increase in permeability is caused by plastic deformation around the cavern, but the pore pressure is also enhanced so that leak-off from the fracture is low. Under those conditions, propagation of large fractures in the Halite cannot be ruled out. Only the permeable layers in the North Sea formation can possibly arrest fracture propagation.

Mitigation of the potential fracture propagation appears impossible with minor changes such as the position of the plug. Putting the plug deeper will reduce the difference between pressure and stress, but only by a few bar. Changing the wait time also has a small effect. It appears that only partial filling up of the cavern would be beneficial, because there would be less energy available for fracture propagation, thereby reducing the volume that could flow out of the cavern over time.

References

Bérest P., Bergues J., Brouard B., Durup J.G. and Guerber B. (2001), “A salt cavern abandonment test.”, Int. J. Rock Mech. & Mining Sci., 38:357-368.

Brouard Consulting (2019), “Over-pressured caverns and leakage mechanisms, Phase 2: Cavern scale”, KEM Study 17, November 2019.

Brouard Consulting (2024), “Convergence and subsidence at cavern ZW-03”, March 2024.

Cleary, M.P., A.R. Crockett and N.M. Okusu, "A complete integrated model for design and real-time analysis of hydraulic fracturing operations.", SPE 15069, presented at the SPE California Regional Meeting in Oakland, CA, April 1986.

Kroon, I.C., B. Orlic, B.C. Scheffers (2003), “Abandonment of solution mined salt caverns in the Netherlands, Part 1 : Review, Part 2: Best Practices and methods”, TNO report, NITG 03-172-B, September 2003.

Nolte, K.G., (1979), "Determination of fracture parameters from fracturing pressure decline", SPE 8341, 54th Annual Technical Conference and Exhibition of the SPE, Las Vegas, NEV.

Rummel F., Benke K. and Denzau H. (1996) Hydraulic Fracturing Stress Measurements in the Krummhörn Gas Storage Field, North-western Germany. Proc. SMRI Spring Meeting, Houston.

Schmidt T. (1993) Fracture Tests for Determining Primary Stress Conditions in Salt Deposits Provide Clues to the Rock Mechanics of Salt Caverns, Proc. 7th Symp. on Salt, Vol I, Elsevier, 135-40.

Staudtmeister K. and Schmidt T. (2000) Comparison of Different Methods for the Estimation of Primary Stresses in Rock Salt Mass with Respect to Cavern Design. Proc. 8th World Salt Symposium, Vol. I, Elsevier, 331-35.

Wawersik W. and Stone C.M. (1989) A characterization of pressure records in inelastic rock demonstrated by hydraulic fracturing measurements in salt. Int. J. Rock Mech. Min. Sci,1989, 613-627.